Research Article Vol. 34, No. 2 / 26 Jan 2026 / Optics Express 2693
Optics EXPRESS

Resolving complex subwavelength grating structures using topologically structured light

THOMAS A. GRANT, ERIC PLUM, NIKOLAY I. ZHELUDEV, AND KEVIN F. MACDONALD*

Optoelectronics Research Centre, University of Southampton, Highfield, Southampton SO17 1BJ, UK
**kfm@orc.soton.ac.uk*

Abstract: It has been seen recently that when probing a nanoscale object to determine, for example, size or position via light scattering, a significant advantage in measurement precision can be gained from exploiting phase singularities in a topologically structured incident light field. Here, we demonstrate that this advantage, derived from the dependence of scattered intensity profiles on strong local (subwavelength-scale) intensity and phase variations in the incident field, can be extended towards imaging applications: analysis of scattering patterns from arbitrary binary gratings under superoscillatory illumination successfully resolves feature sizes down to ~λ/6.6 in single-shot measurements (a factor of 1.3× smaller than is achieved with plane wave illumination), and ~λ/10.5 in positionally-displaced few-shot measurements (which yields no improvement in the plane wave case). Interestingly, there are circumstances in which more complex objects are better resolved than simple structures, because interference effects increase the information content of their scattering patterns.

1. Introduction

Over recent decades, the spatial resolution achievable in far-field optical imaging has advanced well beyond the classical Abbe diffraction limit of ~ λ/2 (where λ is the wavelength of light), through the use of various deterministic, stochastic, and computational signal processing techniques [1–12]. In positional and dimensional optical metrology, techniques based on interferometric free-space light and evanescent field scattering or beam deflection have been developed for tracking isolated (typically optically trapped) nanoparticles with sub-nanometric precision [13–18], and a range of approaches to linear translation measurement with similar precision, leveraging light fields structured at sub-wavelength scales (by metasurfaces, plasmonic nanostructures, and spatial light modulators), have been reported [19–22]. Indeed, precision and accuracy reaching the atomic scale (100-200 pm; < λ/5000) have recently been demonstrated in single-shot optical measurements based on the deep learning analyses of objects' diffraction patterns under illumination by topologically structured light [23–25]. This is made possible by: (a) constraining the problem (i.e., the parameter space within which the inverse scattering problem must be solved, typically using a neural network [26]), e.g., to the retrieval of one, or not more than a few, dimensional parameters from simple, well-defined objects (e.g., the widths and separation of a pair of nano-rods [23], or the 1D position of a nanowire [24]); (b) the fact that the Fisher information content of a nano-object's diffraction pattern can be orders of magnitude larger when it is illuminated with a topologically structured light field containing phase singularities (i.e., high phase and intensity variations with deeply subwavelength scales), as opposed to a plane wave [27].

Here, we examine the extent to which the advantage of topologically structured illumination can be retained in the more challenging task of retrieving dimensional parameters from arbitrarily structured objects, i.e., as the dimensionality of the parameter space grows and feature sizes

#580365 https://doi.org/10.1364/OE.580365
Journal © 2026 Received 26 Sep 2025; revised 1 Dec 2025; accepted 1 Jan 2026; published 21 Jan 2026

Optics EXPRESS

decrease. From single-shot diffraction patterns of random, barcode-like, one-dimensional gratings under superoscillatory illumination, a trained neural network consistently retrieves features down to a size of ~λ/6.6 – a factor of 1.3× smaller than is achieved with plane wave illumination. This advantage is extended to a factor of 2.2× in three-shot superoscillatory imaging (with shot-to-shot object translation), whereby feature sizes down to ~λ/10.5 are resolved. Somewhat counterintuitively, it is found that retrieval success rates can be higher for more complex objects, because interference between light scattered by a greater number of object features increases the information content of the scattered field.

2. Methods

Measuring the position or displacement of a nanowire as reported in Refs. [24,25] is a task that can be identically described as retrieving the dimensions of a double slit: i.e., the widths A and B of slits on either side of the nanowire, under the constraint that A + B is constant. As target objects for the present computational study, we consider random grating patterns comprising an arbitrary number of transparent slits in an otherwise perfectly opaque, absorbing, zero-thickness screen, illuminated with monochromatic light at a wavelength λ = 488 nm (Fig. 1). We generate a set of 4096 different grating profiles, each 10 μm long with 10 nm pixelation in the x direction and 1 μm wide in y, centered within a 40 μm × 40 μm illuminated screen area, as follows: In each case, the first pixel is set as either transparent or opaque with equal probability; Subsequent pixels then either adopt the same state or change to the opposing state with a probability randomly sampled from a flat distribution of values from 0.01 to 0.11; After any change from transparent to opaque or vice versa, a new change probability is selected. This ensures that feature sizes (meaning the distance between any two changes of state - see Fig. 2(a)) within a single pattern, and across the whole set of patterns, are uncorrelated but span a range of values of interest around and below the classical diffraction limit (from ~λ/2 down to λ/50).

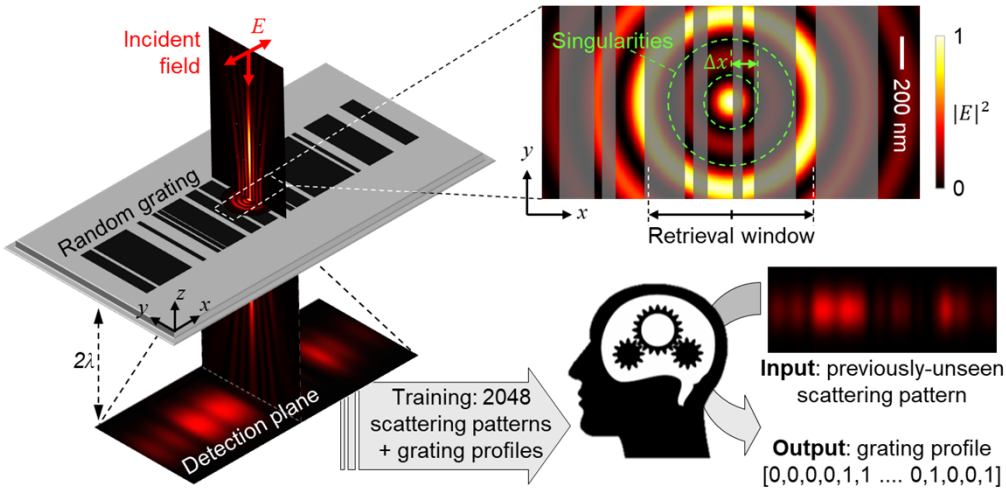

Fig. 1. Dimensional profiles of the central (1 μm wide) section of arbitrary, randomly generated binary gratings are retrieved via a deep learning-enabled analysis of their transmission scattering patterns. N.B. the schematic on the left of this figure is not to scale: in practice, the incident field and the screen extend to a 40 μm × 40 μm area much larger than the (10 μm × 1 μm) gratings. The zoomed section top right shows the central region of the incident superoscillatory field profile to scale against a representative section of grating.

We assume the gratings are illuminated with an axially symmetric superoscillatory light field [28,29], as used in a number of recent experimental studies [23–25], described by a

Optics EXPRESS

linear combination of two band-limited, prolate spheroidal wave functions (see Supplement 1): $\tilde{U}(r/\lambda) = [21.65S_2(r/\lambda) + S_3(r/\lambda)]$, where r is the distance from the beam axis. This gives an incident field profile with a central intensity peak of 0.3λ half-maximum width, flanked by a series of phase singularities. Taking this to be centered on the gratings, their transmission scattering patterns at a distance 2λ beyond the sample are calculated using the angular spectrum method, assuming a 5.12 μm × 1.28 μm field of view with 10 nm pixelation (again, in keeping with achievable magnification, and therefore effective pixel size, in experiments [23–25]). From these scattering patterns we seek to retrieve the dimensional profile of the central 1 μm-long section of the grating, in the form of a 1×100 vector of zeros (=opaque) and ones (=transparent). To this end, half of the set of 4096 scattering patterns and corresponding grating profiles, selected at random, are used for training and validation of a convolutional neural network (see Supplement 1 for details of network architecture and training). The other 2048 scattering patterns are then used

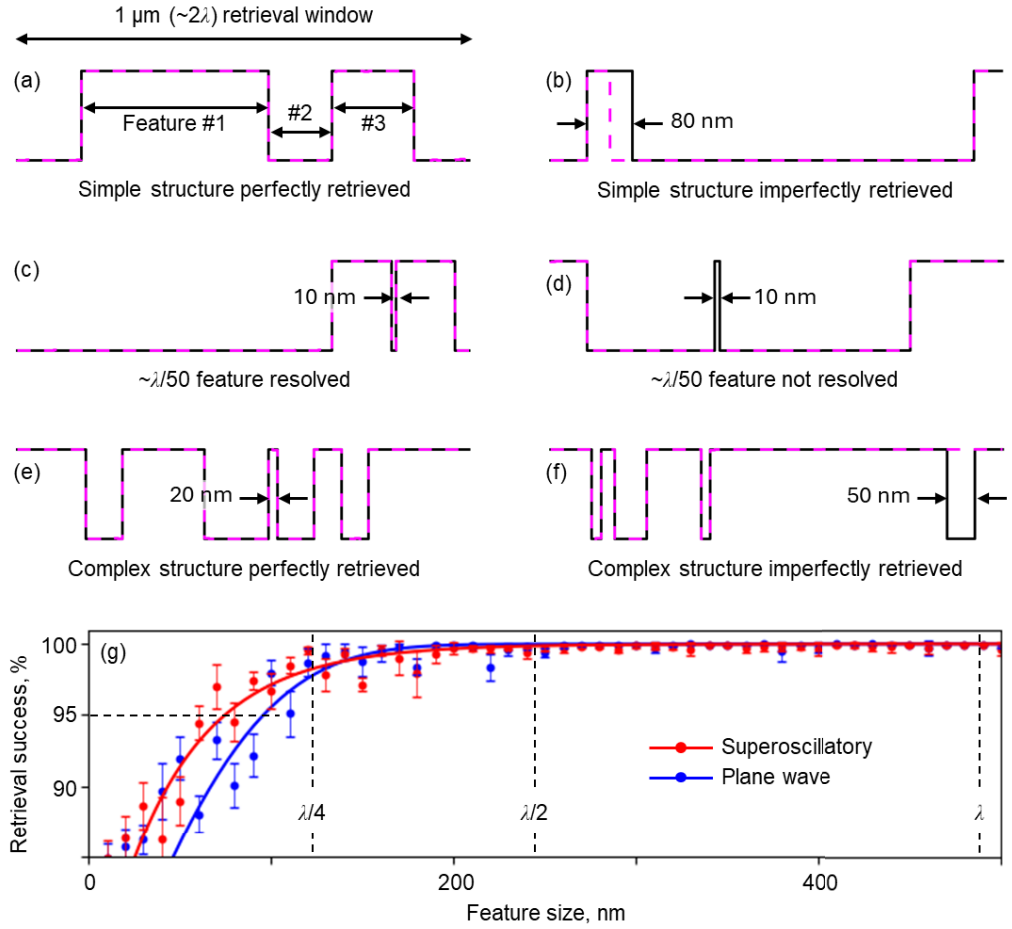

Fig. 2. (a)–(f) Illustrative examples of perfect and imperfect grating profile retrieval with superoscillatory illumination, for profiles of varying complexity, containing features of varying size. Solid black lines are the true grating profiles, pink dashed lines are optically retrieved profiles. (g) Retrieval success as a function of feature size for plane wave and superoscillatory illumination. Points and error bars represent respectively the mean and standard deviation of results from ten independently trained networks each tested on the same set of 2048 previously unseen scattering patterns. [Line fittings have the form of shifted Weibull distributions.]

Optics EXPRESS

for testing, i.e., as unseen patterns for nominally unknown grating profiles. For comparison, the exercise is repeated for plane wave (i.e., unstructured) illumination, using the same set of gratings split into the same training/validation and testing subsets. In both cases, results are aggregated over ten neural network training and testing cycles, whereby the random assignment of scattering patterns to the training and validation subsets is different each time.

3. Results

Figures 2(a)–(f) show an illustrative selection of retrieved vs. actual grating profiles, including: relatively simple and sparse profiles (a, b) – i.e., containing a small number of well-separated feature 'edges' (transparent/opaque transitions); profiles containing few but closely-spaced edges (c, d) – i.e., very narrow features, down to ~λ/50 wide; and more complex profiles containing a higher numbers of features with a variety of dimensions (e, f).

For direct imaging methods, the Rayleigh criterion is used to define resolution [30]. However, this is not appropriate for a probabilistic multi-parameter retrieval problem, since retrieving a feature of a certain size in one case does not imply that features of that size will be retrieved in all cases (e.g., compare Figs. 2(c), (d)). As such, we quantify resolving power in terms of the mean rate at which pixels are correctly retrieved, as a function of the size of the feature within which they are located (Fig. 2(g)). Retrieval is all but perfect for feature sizes above the classical ~λ/2 diffraction limit, with both plane wave and superoscillatory illumination. Below this, smaller features can be resolved in both cases because interference between light scattered by different object features translates information about short length-scale structure into that part of the angular spectrum which propagates into the far-field, and the neural network training process provides a deconvolution mechanism to access that information. A retrieval success rate >95% is maintained with plane wave illumination down to feature sizes of 95 nm (~λ/5.1), and with superoscillatory illumination down to 74 nm (λ/6.6).

The enhancement of resolution in the superoscillatory case, by a factor of ~1.3, is explained by the greater Fisher information [31,32] content of the more complex scattered field, arising from the presence of high local (subwavelength scale) intensity and phase variations in the incident field interacting with the object, particularly in the vicinity of phase singularities [27]. The increased complexity of the scattering pattern does however also make the retrieval problem more challenging, and this is reflected in neural network learning rates: With superoscillatory illumination, the network takes more epochs to converge but does so to a lower mean squared error (see Supplement 1), thereby ultimately yielding higher retrieval success rates for smaller feature sizes.

Greater superoscillatory advantage can be gained from the fact that diffraction patterns of topologically structured light are highly sensitive to changes in the mutual positions of object features (e.g., grating slit edges) and incident field features (esp. phase singularities). Indeed, it has been demonstrated that this sensitivity can provide for optical localization of a known single nano-object with picometric (i.e., atomic scale) precision at visible wavelengths [24,25]. Thus, for the purposes of parameter retrieval from arbitrary objects, scanning or multi-shot recording of diffraction patterns (i.e., with known shot-to-shot translation between the incident superoscillatory beam and the object) will provide additional information for neural network training and subsequent retrieval of grating profiles from unseen scattering patterns. Figure 3 shows how retrieval performance is enhanced through the use of just two additional diffraction patterns, recorded for incident beam displacements of ±Δx (where Δx is equal to the distance between the beam axis and the first singularity in the radial profile, 160 nm in the present case, ~λ/3 – see Fig. 1). In this case, the 95% threshold for successfully resolving grating features extends down to ~λ/10.5 (47 nm). No such enhancement of performance is possible under plane wave illumination because scattering patterns in that case are invariant with respect to translation of the incident field.

Optics EXPRESS

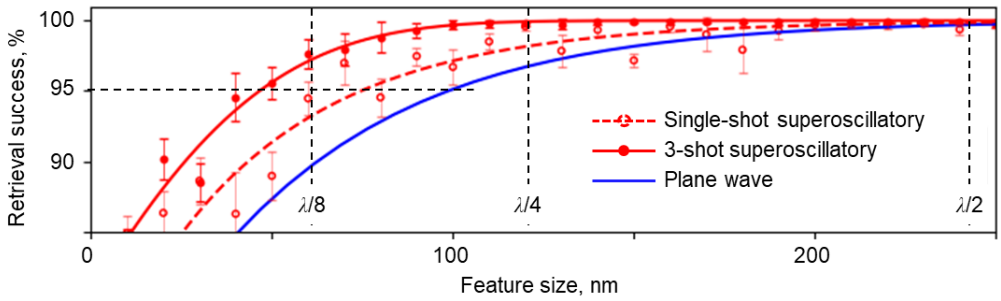

Fig. 3. Retrieval success as a function of feature size for single- and 3-shot superoscillatory illumination of gratings. In the single-shot case, the incident beam is centered at (0,0). In the 3-shot case, additional diffraction patterns are recorded at beam positions $\pm\Delta x \sim\lambda/3$. Points and error bars represent respectively the mean and standard deviation of results from ten independently trained networks. (Line fittings have the form of shifted Weibull distributions. The trend line for plane wave illumination from Fig. 2 is overlaid for reference.)

Thus far, we have considered retrieval performance only as a function of feature size, regardless to the complexity of the grating, i.e., the number of features within the 1 μm retrieval window. Interestingly, single-shot retrieval performance is found to be better – meaning smaller features are retrieved with greater success – for more complex objects (Fig. 4).

Here, neural networks are trained and validated as before, using half of the full set of 4096 scattering patterns (encompassing all feature sizes and gratings of all complexity levels), then tested separately on gratings defined as either 'simple' – presenting between one and three features of any size within the retrieval window (i.e., 2-4 opaque/transparent transitions), or 'complex' – presenting four or more features (only ~6% of gratings present ≥8 features; none present >12 features). This divides the test set into approximately equal numbers of unseen scattering patterns for simple and complex gratings, enabling a statistically fair comparison (~20% of grating profiles contain only a single edge or none, i.e., do not include a complete 'feature', and are therefore excluded from this comparison). We attribute the simple vs. complex performance differential, which is greater for plane wave than for superoscillatory illumination, to the fact that the flow of Fisher information from the object (grating) plane to the detection plane is controlled by interference (as of course is optical power flow, but the two do not generally coincide because their sources do not coincide [32,33]): Information from a given feature in the object plane is better projected onto the detected intensity field (over a finite aperture in the detection plane) when there are other features nearby [34]. The improvement in retrieval success with grating complexity obviously cannot continue indefinitely: with finite detector resolution and finite dataset size, and where increasing complexity equates to decreasing feature size (within a finite retrieval window), there must come a point where the deconvolution mechanism fails. Indeed, as shown in Fig. 2(g), retrieval success falls rapidly (regardless of grating complexity) for feature sizes $<\lambda/10$.

Optics EXPRESS

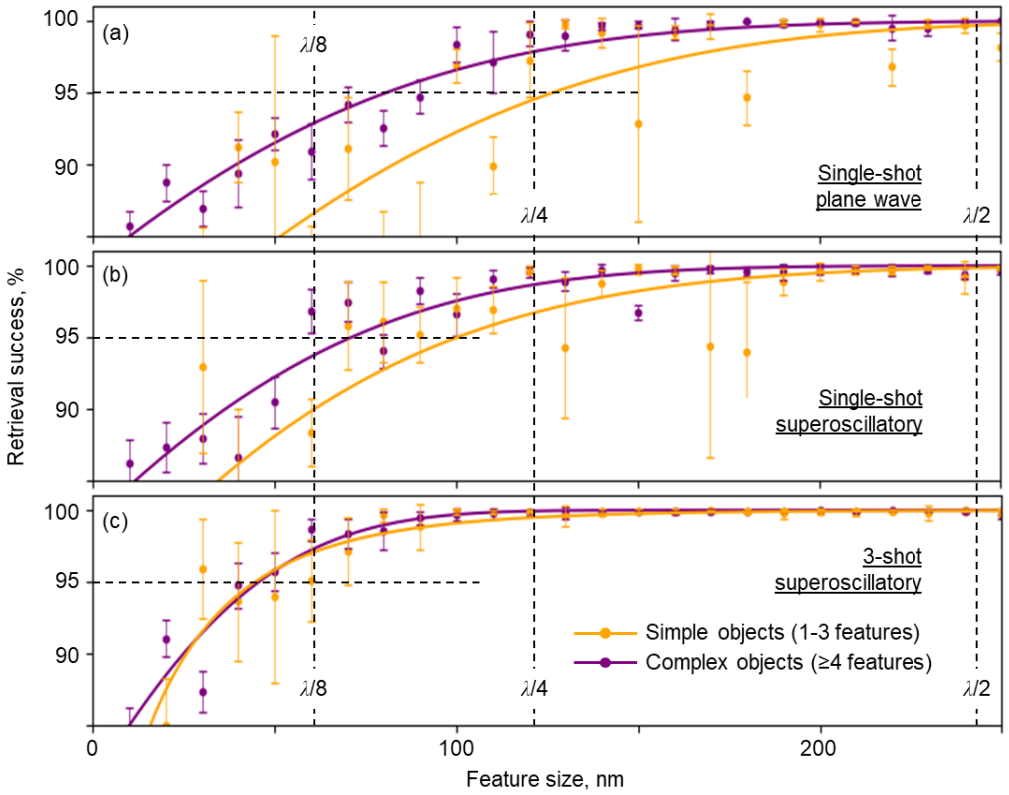

Fig. 4. Retrieval success as a function of feature size for simple gratings [presenting 1-3 features within the 1 μm retrieval window – orange points and trend lines] and complex gratings [≥4 features – purple points and trend lines] for (a) single-shot plane wave, (b) single-shot superoscillatory, (c) 3-shot superoscillatory illumination. Points and error bars represent respectively the mean and standard deviation of results from ten independently trained networks. Line fittings have the form of shifted Weibull distributions.

4. Conclusion

In summary, we have shown here that the advantages of topologically structured illumination (over plane wave illumination), previously seen in scattering-based optical metrology, can be maintained when the dimensional parameter space expands from that of a tightly-constrained single value retrieval task to that of retrieving an unspecified number of parameters from a complex object. Despite the increased complexity of the parameter estimation problem, neural networks can establish a deconvolution algorithm which leverages an enhancement of information content in scattering patterns derived from the interaction of strong local intensity and phase variations in the incident field with nanometric features of the scattering object. Single-shot resolution down to λ/6.6 is achieved in retrieval of random binary grating profiles under superoscillatory illumination, improving to λ/10.5 in few-shot imaging (beating plane wave illumination by a factor of 2.2×). These results open a path to the use of topologically structured light for increasingly complex nanoscale optical measurement and basic (e.g., binary object) imaging tasks.

The practical constraints on realizing this ‘superoscillatory advantage’, for gratings or any other nanostructure, will lie in the accuracy of fabrication and ground truth dimensional labelling of training samples (i.e., in the fidelity of lithographic manufacturing and resolution of electron microscopic imaging), the accuracy and reproducibility of alignment between samples and the

Optics EXPRESS

incident structured light field, and in detector shot noise. It has been shown experimentally that forms of systematic noise manifesting at the image-to-image level (e.g., instrumental thermomechanical fluctuation, even at scales much larger than the dimensions or displacements being measured) can be very effectively excluded by suitable iteration of training data collection [25], but shot noise occurs at the pixel-to-pixel level within each scattering pattern. Robustness against the latter can be assessed by adding Poissonian noise to simulated scattering patterns (normalized to a specified whole-dataset single-pixel maximum photon count - see Supplement 1): in the presence of noise, the network converges to a mean squared error matching the ideal (noise-free) case when said brightest-pixel photon count is greater than $\sim 10^3$ – a level commensurate with the full well capacity of mid-range imaging sensors.

Funding. Engineering and Physical Sciences Research Council (EP/T02643X/1, EP/Z53285X/1).

Disclosures. The authors declare no conflicts of interest.

Data availability. All information necessary to reproduce the results presented is contained within the article.

Supplemental document. See Supplement 1 for supporting content.

References

1. F. Balzarotti, Y. Eilers, K. C. Gwosch, *et al.*, "Nanometer resolution imaging and tracking of fluorescent molecules with minimal photon fluxes," Science **355**(6325), 606–612 (2017).
2. G. Barbastathis, A. Ozcan, and G. Situ, "On the use of deep learning for computational imaging," Optica **6**(8), 921–943 (2019).
3. E. Betzig, G. H. Patterson, R. Sougrat, *et al.*, "Imaging intracellular fluorescent proteins at nanometer resolution," Science **313**(5793), 1642–1645 (2006).
4. S. Gazit, A. Szameit, Y. C. Eldar, *et al.*, "Super-resolution and reconstruction of sparse sub-wavelength images," Opt. Express **17**(26), 23920–23946 (2009).
5. J. M. Guerra, "Super-resolution through illumination by diffraction-born evanescent waves," Appl. Phys. Lett. **66**(26), 3555–3557 (1995).
6. M. G. L. Gustafsson, "Nonlinear structured-illumination microscopy: Wide-field fluorescence imaging with theoretically unlimited resolution," Proc. Natl. Acad. Sci. U.S.A. **102**(37), 13081–13086 (2005).
7. S. W. Hell and J. Wichmann, "Breaking the diffraction resolution limit by stimulated emission: stimulated-emission-depletion fluorescence microscopy," Opt. Lett. **19**(11), 780–782 (1994).
8. Y. Rivenson, Y. Zhang, H. Günaydın, *et al.*, "Phase recovery and holographic image reconstruction using deep learning in neural networks," Light: Sci. Appl. **7**(2), 17141 (2017).
9. M. J. Rust, M. Bates, and X. Zhuang, "Sub-diffraction-limit imaging by stochastic optical reconstruction microscopy (STORM)," Nat. Methods **3**(10), 793–796 (2006).
10. Y. Shechtman, Y. C. Eldar, O. Cohen, *et al.*, "Phase Retrieval with Application to Optical Imaging: A contemporary overview," IEEE Signal Process. Mag. **32**(3), 87–109 (2015).
11. A. Sinha, J. Lee, S. Li, *et al.*, "Lensless computational imaging through deep learning," Optica **4**(9), 1117–1125 (2017).
12. A. Szameit, Y. Shechtman, E. Osherovich, *et al.*, "Sparsity-based single-shot subwavelength coherent diffractive imaging," Nat. Mater. **11**(5), 455–459 (2012).
13. H. Ma, Y. Zhang, J. Zhou, *et al.*, "Infinitesimal optical singularity ruler for three-dimensional picometric metrology," Nat. Commun. **15**(1), 10853 (2024).
14. P. Maurer, C. Gonzalez-Ballestero, and O. Romero-Isart, "Quantum theory of light interaction with a Lorenz-Mie particle: Optical detection and three-dimensional ground-state cooling," Phys. Rev. A **108**(3), 033714 (2023).
15. L. Wei, A. V. Zayats, and F. J. Rodríguez-Fortuño, "Interferometric Evanescent Wave Excitation of a Nanoantenna for Ultrasensitive Displacement and Phase Metrology," Phys. Rev. Lett. **121**(19), 193901 (2018).
16. Y. Xu, B. Gao, A. He, *et al.*, "An ultra-compact angstrom-scale displacement sensor with large measurement range based on wavelength modulation," Nanophotonics **11**(6), 1167–1176 (2022).
17. G. H. Yuan and N. I. Zheludev, "Detecting nanometric displacements with optical ruler metrology," Science **364**(6442), 771–775 (2019).
18. H. Zang, Z. Zhang, Z. Huang, *et al.*, "High-precision two-dimensional displacement metrology based on matrix metasurface," Sci. Adv. **10**(2), eadk2265 (2024).
19. M. Facchin, S. N. Khan, K. Dholakia, *et al.*, "Determining intrinsic sensitivity and the role of multiple scattering in speckle metrology," Nat. Rev. Phys. **6**(8), 500–508 (2024).
20. C. Gonzalez-Ballestero, M. Aspelmeyer, L. Novotny, *et al.*, "Levitodynamics: Levitation and control of microscopic objects in vacuum," Science **374**(6564), eabg3027 (2021).
21. R. Huang, I. Chavez, K. M. Taute, *et al.*, "Direct observation of the full transition from ballistic to diffusive Brownian motion in a liquid," Nat. Phys. **7**(7), 576–580 (2011).

Optics EXPRESS

22. T. Li, S. Kheifets, D. Medellin, *et al.*, "Measurement of the Instantaneous Velocity of a Brownian Particle," Science **328**(5986), 1673–1675 (2010).
23. T. Pu, J. Y. Ou, V. Savinov, *et al.*, "Unlabeled Far-Field Deeply Subwavelength Topological Microscopy (DSTM)," Adv. Sci. **8**(1), 2002886 (2021).
24. T. Liu, J. Y. Ou, J. Xu, *et al.*, "Picophotonic localization metrology beyond thermal fluctuations," Nat. Mater. **22**(7), 844–847 (2023).
25. C. H. Chi, E. Plum, N. I. Zheludev, *et al.*, "Robust Optical Picometrology Through Data Diversity," Opt. Mater. Express **14**(10), 2377–2383 (2024).
26. V. Vemuri and G.-S. Jang, "Inversion of Fredholm integral equations of the first kind with fully connected neural networks," J. Frankl. Inst. **329**(2), 241–257 (1992).
27. T. A. Grant, A. N. Vetlugin, E. Plum, *et al.*, "Localization of nanoscale objects with light singularities," Nanophotonics **14**(7), 915–920 (2025).
28. N. I. Zheludev, "What diffraction limit?" Nat. Mater. **7**(6), 420–422 (2008).
29. K. S. Rogers, K. N. Bourdakos, G. H. Yuan, *et al.*, "Optimising superoscillatory spots for far-field super-resolution imaging," Opt. Express **26**(7), 8095–8112 (2018).
30. Rayleigh, "XXXI. Investigations in optics, with special reference to the spectroscope," The London, Edinburgh, and Dublin Philosophical Magazine and J. Science **8**(49), 261–274 (1879).
31. S. Kay, *Fundamentals of Statistical Processsing: Estimation Theory* (Prentice Hall, 1993).
32. J. Hüpfl, F. Russo, L. M. Rachbauer, *et al.*, "Continuity equation for the flow of Fisher information in wave scattering," Nat. Phys. **20**(8), 1294–1299 (2024).
33. M. Weimar, H. Zhou, L. Neubacher, *et al.*, "Controlling the Flow of Information in Optical Metrology," arXiv (2025).
34. C. H. Chi, T. Grant, K. F. MacDonald, *et al.*, "Resolution Beyond λ/10,000 in Single-Shot Optical Localization Metrology," in *Frontiers in Optics + Laser Science* (2025).